Radiation flow and viscous stresses in anisotropic gravitational collapse

Justino Martínez,[1] Diego Pavón[1] and Luis A. Núñez[2]

[1] *Grupo de Física Estadística, Dept. de Física, Universidad Autónoma de Barcelona, 08193 Bellaterra, Barcelona, Spain*
[2] *Laboratorio de Física Teórica, Dept. de Física, Universidad de Los Andes, Mérida 5101, Venezuela*

ABSTRACT
The Herrera–Jiménez–Ruggeri method is employed to analyse the evolution of anisotropic radiating fluid spheres endowed with viscous stresses. The growth of the anisotropy with the distance to the centre allows us to divide the sphere interior into three concentric zones, which differ from each other in the degree of interaction between matter and radiation. The compression wave plays a greater role in the dynamics than it does in the isotropic case. Other effects are also considered in detail.

Key words: gravitation – hydrodynamics – radiative transfer – relativity – stars: mass-loss – stars: neutron.

1 INTRODUCTION

In many instances, giant stars and compact objects like neutron stars are partners in binary systems. During their evolution the giant component may overcome the Roche lobe, losing mass to its companion. In some cases, the mass engulfed by the neutron star may destabilize it, triggering a highly relativistic collapse. Also highly relativistic is the collapse of the neutron star left over in supernovae explosions. The dynamics of collapsing, dense stars is deeply influenced by the opacity of their core (Kazanas 1978; Kazanas & Schramm 1979; Shapiro & Teukolsky 1983; Bruenn 1985; Demiański 1985; Bahcall 1989). At very high densities the neutrinos get trapped in it; this strongly reduces the luminosity of the star and greatly affects the thermodynamic quantities within the fluid. The maximum attainable temperature during collapse is about 10^{11} to 10^{12} K, and the cooling necessary to recover the equilibrium is obtained by neutrino emission which, at those high densities, becomes dominated by the neutronization reaction $e^- + p \rightarrow \nu_e + n$ (Shapiro & Teukolsky 1983; Bruenn 1985; Demiański 1985; Bahcall 1989). In the core, the equilibrium between matter and radiation is governed by the absorption and emission of neutrinos and antineutrinos on free nucleons, and from the nucleon absorption, $\nu_e + n \rightarrow e^- + p$; the latter turns out to be the most important source of neutrino opacity.

Another important aspect, though frequently overlooked in the literature, refers to viscosity. In fact, the viscous part of the stress-energy tensor does not vanish in general for a mixture of radiation and matter (Weinberg 1971), and so a realistic treatment of gravitational collapse should take it into account (Santos 1984; Barreto & Rojas 1992; Martínez & Pavón 1994). Viscosity can be understood as a phenomenological consequence of the exchange of momentum between the different layers of the star; hence it inevitably arises in the star core because of the intimate interaction between radiation and matter there. The existence of shear viscosity increases the anisotropy of the system. In some neutron stars, the exotic phase transition (Sawyer & Scalapino 1973), the solid–liquid coexistence due to the presence of a crust (Ruderman 1972), and the superfluid–normal fluid transition due to the presence of a superfluid state are sources of anisotropy as well.

In this paper, we use the Herrera–Jiménez–Ruggeri method (Herrera, Jiménez & Ruggeri 1980, hereafter HJR) to obtain non-static solutions to the Einstein equations for a radiating fluid with viscous pressure. The radiating fluid viscous sphere is properly matched to the Vaidya exterior metric, and the evolution of the sphere is restricted by regularity conditions, by a heuristic assumption relating density, pressure and radial matter velocity, and by a physical description of the radiation-hydrodynamic scenario. This *ansatz*, guided by solid physical principles, reduces the problem of solving Einstein equations to a numerical integration of a system of ordinary differential equations for quantities evaluated at the boundary surface. This method has been used to model a variety of situations: anisotropic collapse (Cosenza et al. 1982), propagation of shock waves (Herrera & Núñez 1990), viscous process in the diffusion approximation (Barreto & Rojas 1992), radially oscillating stars (Aquilano, Barreto & Núñez 1994), collapse of slowly rotating stars (Herrera et al. 1994), and others (Barreto & Núñez 1991; Aguirre, Hernández & Núñez 1994). We assume the system to be composed of matter and radiation, and the degree of interaction between them to be non-uniform throughout the star. The evolution of the inner regions is governed by the diffusion process, while in the crust the situation is reversed, since the interaction between matter and radiation there is almost non-existent. In this context, there are two distinct contributions to the anisotropy of

the system: the non-diffusive radiation and the shear viscous pressure. As it turns out, both viscosity coefficients present the same behaviour and order of magnitude. Shortly after the beginning of the collapse, a compression wave builds up at the centre of the star, which on its way outward deeply affects the evolution of the system. As the surface falls down, an interesting effect takes place. The material just beneath it reverses its radial velocity and eventually starts to travel outwards.

This paper is organized as follows. In Section 2, the anisotropic stress-energy tensor for a non-comoving observer in Bondi coordinates is constructed. In Section 3, the Einstein equations are presented. These, together with the junction conditions and surface equations (Section 4), allow us to find four quantities which govern the collapse. Nevertheless, in the case of anisotropic collapse, an additional equation is needed to solve the field equations. This equation, which links radial to tangential pressure, is introduced following Cosenza et al. (1981, 1982). In Section 5, to find the radiation energy density and the viscosity coefficients, we assume a very simple structure for the star. It consists of three differentiated zones: the core in which the opacity of the matter is very high; the most external part of the star, the crust, in which the radiation practically does not interact with matter, and consequently viscous stresses vanish there; and an intermediate zone, located between these two, which smoothly connects them. This is illustrated by means of an example. Finally, the last section summarizes the results of this work. To illustrate them, the differences between this anisotropic model and the isotropic one, i.e. radiation in the diffusion regime throughout the star and vanishing shear viscosity, are presented.

We adopt metrics of signature -2. The quantities subscripted with 'a' denote that they are evaluated at the surface. The subscripts 0 and 1 indicate partial differentiation with respect to time (u) and radial coordinate (r), respectively.

2   STRESS-ENERGY TENSOR

We consider a sphere composed of a material medium plus radiation. Thus the stress-energy tensor, as seen by a local Minkowskian observer comoving with the fluid, splits into three terms: a material term, $\hat{T}_{\mu\nu}^{M}$, a radiation term, $\hat{T}_{\mu\nu}^{R}$, and a third term, $\hat{T}_{\mu\nu}^{V}$, which reports the viscous character of the matter–radiation interaction of the fluid. The comoving *Minkowskian* observer coincides with the *Lagrangian frame* (the *proper frame*), which is the frame where the interaction between radiation and matter is most easily handled (Mihalas & Mihalas 1984). The physical variables are obtained as measured by this observer, and the effects of gravitation are clearly provided through the appropriate transformation to a curvilinear coordinate system.

For the above local comoving observer the material part of the stress-energy tensor has the form

$$\hat{T}_{\mu\nu}^{M} = (\rho_{M} + P)\, \hat{U}_{\mu} \hat{U}_{\nu} - P\eta_{\mu\nu},$$

and the viscous part has the form

$$\hat{T}_{\mu\nu}^{V} = \hat{\tau}_{\mu\nu} = \hat{\pi}_{\mu\nu} + \Pi P_{\mu\nu},$$

where $\hat{\pi}_{\mu\nu}$ denotes the traceless viscous pressure tensor, $P_{\mu\nu} = \eta_{\mu\nu} - \hat{U}_{\mu} \hat{U}_{\nu}$ is the spatial projection tensor, and Π is the bulk viscous pressure.

The radiation portion of the stress-energy tensor reads (Lindquist 1966; Mihalas & Mihalas 1984)

$$\hat{T}_{\mu\nu}^{R} = \begin{pmatrix} \rho_{R} & -\mathscr{F} & 0 & 0 \\ -\mathscr{F} & \mathscr{P} & 0 & 0 \\ 0 & 0 & \mathscr{P}_{\perp} & 0 \\ 0 & 0 & 0 & \mathscr{P}_{\perp} \end{pmatrix},$$

where $\mathscr{F}$ denotes the radiation energy density flow, ρ_{R} the radiation energy density, $\mathscr{P}$ the radiation pressure, and $\mathscr{P}_{\perp} = \frac{1}{2}(\rho_{R} - \mathscr{P})$. These quantities are the moments of the *specific intensity of radiation*, $I(x, t; \boldsymbol{n}, \nu)$, which for a planar geometry can be written as

$$\rho_{R} = \frac{1}{2} \int_{0}^{\infty} d\nu \int_{-1}^{1} d\mu\, I(x, t; \boldsymbol{n}, \nu), \tag{1}$$

$$\mathscr{F} = \frac{1}{2} \int_{0}^{\infty} d\nu \int_{-1}^{1} d\mu\, \mu I(x, t; \boldsymbol{n}, \nu) \tag{2}$$

and

$$\mathscr{P} = \frac{1}{2} \int_{0}^{\infty} d\nu \int_{-1}^{1} d\mu\, \mu^{2} I(x, t; \boldsymbol{n}, \nu), \tag{3}$$

where $\mu = \cos\theta$. In classical radiative transfer theory, the specific intensity of the radiation field, $I(x, t; \boldsymbol{n}, \nu)$, at the position x and time t, travelling in the direction $\boldsymbol{n}$ with a frequency ν, is defined so that

$$d\mathscr{E} = I(x, t; \boldsymbol{n}, \nu)\, dS \cos\alpha\, d\vartheta\, d\nu\, dt \tag{4}$$

is the energy crossing a surface element dS, into solid angle $d\vartheta$ around $\boldsymbol{n}$ (α is the angle between $\boldsymbol{n}$ and the normal to dS), transported by radiation of frequencies $(\nu, \nu + d\nu)$, in time dt (see Mihalas & Mihalas 1984 for details).

Finally, the dissipative terms in the stress-energy tensor, $\Delta \hat{T}_{\mu\nu}$, must satisfy the relation $\Delta \hat{T}_{\mu\nu} \hat{U}^{\mu} \hat{U}^{\nu} = 0$. Applying this condition to the viscous part of the stress-energy tensor, and using the traceless condition of $\hat{\pi}_{\mu\nu}$, we obtain

$$\hat{\pi}_{\mu\nu} = \begin{pmatrix} 0 & 0 & 0 & 0 \\ 0 & \pi & 0 & 0 \\ 0 & 0 & -(\pi/2) & 0 \\ 0 & 0 & 0 & -(\pi/2) \end{pmatrix}.$$

Thus, for a local observer with radial velocity ω, comoving with the fluid, the stress-energy tensor in local Minkowskian coordinate takes the form

$$\hat{T}_{\mu\nu} = (\rho + P_{\perp})\, \hat{U}_{\mu} \hat{U}_{\nu} - P_{\perp} \eta_{\mu\nu}$$
$$+ (P_{r} - P_{\perp})\, \hat{\chi}_{\mu} \hat{\chi}_{\nu} - \hat{\mathscr{F}}_{\mu} \hat{U}_{\nu} - \hat{\mathscr{F}}_{\nu} \hat{U}_{\mu},$$

with

$$\hat{U}_{\mu} = (1, 0, 0, 0),$$

$$\hat{\chi}_{\mu} = (0, 1, 0, 0),$$

$$\hat{\mathscr{F}}_{\mu} = (0, \mathscr{F}, 0, 0),$$

$$P_{r} = P + \mathscr{P} + \Pi + \pi, \tag{5}$$

$$P_{\perp} = P_{r} + \frac{1}{2}(\rho_{R} - 3\mathscr{P}) - \frac{3}{2}\pi. \tag{6}$$

Now, by applying a Lorentz boost in the radial direction we obtain the stress-energy tensor in Minkowskian coordinates as seen by a non-comoving observer,

$$\bar{T}_{\mu\nu} = L_\mu^\alpha(-\omega)\, L_\nu^\beta(-\omega)\, \hat{T}_{\alpha\beta}.$$

Under this transformation the stress-energy tensor can be written as

$$\bar{T}_{\mu\nu} = (\rho + P_\perp)\, \bar{U}_\mu \bar{U}_\nu - P_\perp\, \eta_{\mu\nu}$$
$$+ (P_r - P_\perp)\, \bar{\chi}_\mu \bar{\chi}_\nu - \bar{\mathscr{F}}_\mu \bar{U}_\nu - \bar{\mathscr{F}}_\nu \bar{U}_\mu,$$

where

$$\bar{U}_\mu = \gamma(1, -\omega, 0, 0),$$
$$\bar{\chi}_\mu = \gamma(-\omega, 1, 0, 0),$$
$$\bar{\mathscr{F}}_\mu = \gamma \mathscr{F}(-\omega, 1, 0, 0),$$
$$\gamma = (1 - \omega^2)^{-1/2}.$$

A further transformation allows us to express the stress-energy tensor in curvilinear coordinates,

$$T_{\mu\nu} = \Lambda_\mu^\alpha \Lambda_\nu^\beta \bar{T}_{\alpha\beta}, \tag{7}$$

where Λ_μ^α is a coordinate transformation matrix which connects Minkowskian to curvilinear coordinates.

In radiation coordinates (Bondi 1964) the interior metric takes the form

$$ds^2 = e^{2\beta}\left(\frac{V}{r}\, du^2 + 2\, du\, dr\right) - r^2(d\theta^2 + \sin^2\theta\, d\phi^2). \tag{8}$$

In the last equation, $u = x^0$ is a time-coordinate, $r = x^1$ is the null coordinate, and $\theta = x^2$ and $\phi = x^3$ are the usual angle coordinates. The u-coordinate is the retarded time in flat space–time, and u-constant surfaces are therefore null cones open to the future. The metric variables β and V in equation (8) are functions of u and r. A function $\tilde{m}(u, r)$ can be defined by

$$V = e^{2\beta}[r - 2\tilde{m}(u, r)], \tag{9}$$

which is the generalization, inside the distribution, of the 'mass aspect' defined by Bondi, Van der Burg & Metzner (1962). In the static limit it coincides with the Schwarzschild mass. In order to give a clear physical significance to the above formulae, we now introduce local Minkowski coordinates (t, x, y, z), which are related to Bondi's radiation coordinates by

$$dt = e^\beta\left(\sqrt{\frac{V}{r}}\, du + \sqrt{\frac{r}{V}}\, dr\right),$$

$$dx = e^\beta \sqrt{\frac{r}{V}}\, dr,$$

$$dy = r\, d\theta,$$

$$dz = r \sin\theta\, d\phi, \tag{10}$$

and to the Schwarzschild coordinates (T, R, Θ, Φ) by

$$T = u + \int_0^r \frac{r}{V}\, dr,$$

$$R = r, \qquad \Theta = \theta, \qquad \Phi = \phi. \tag{11}$$

Now, applying (7), we obtain

$$T_{\mu\nu} = (\rho + P_\perp)\, U_\mu U_\nu - P_\perp\, g_{\mu\nu}$$
$$+ (P_r - P_\perp)\, \chi_\mu \chi_\nu - \mathscr{F}_\mu U_\nu - \mathscr{F}_\nu U_\mu,$$

where

$$U_\mu = e^\beta\left(\sqrt{\frac{V}{r}}\frac{1}{(1-\omega^2)^{1/2}}, \quad \sqrt{\frac{r}{V}}\left(\frac{1-\omega}{1+\omega}\right)^{1/2}, \quad 0, \quad 0\right),$$

$$\chi_\mu = e^\beta\left(-\sqrt{\frac{V}{r}}\frac{\omega}{(1-\omega^2)^{1/2}}, \quad \sqrt{\frac{r}{V}}\left(\frac{1-\omega}{1+\omega}\right)^{1/2}, \quad 0, \quad 0\right),$$

$$\mathscr{F}_\mu = \mathscr{F}e^\beta\left(-\sqrt{\frac{V}{r}}\frac{\omega}{(1-\omega^2)^{1/2}}, \quad \sqrt{\frac{r}{V}}\left(\frac{1-\omega}{1+\omega}\right)^{1/2}, \quad 0, \quad 0\right).$$

Note that

$$\mathscr{F}^\mu U_\mu = 0.$$

For this non-comoving observer the stress-energy tensor in Bondi coordinates is

$$e^{-2\beta}\frac{r}{V} T_{uu} = \frac{1}{1-\omega^2}(\rho + 2\omega\mathscr{F} + P_r\,\omega^2), \tag{12}$$

$$e^{-2\beta} T_{ur} = \frac{1}{1+\omega}[\rho - \mathscr{F}(1-\omega) - P_r\,\omega], \tag{13}$$

$$e^{-2\beta}\frac{V}{r} T_{rr} = \frac{1-\omega}{1+\omega}(\rho - 2\mathscr{F} + P_r), \tag{14}$$

$$T_\theta^\theta = T_\phi^\phi = -P_\perp. \tag{15}$$

Outside matter the metric is the Vaidya one, a particular case of the Bondi metric in which $\beta = 0$ and $V = r - 2\tilde{m}$; the stress-energy tensor corresponds to that of a null fluid, i.e.

$$T_{\mu\nu} = \varepsilon k_\mu k_\nu,$$

where

$$k_\mu = \delta_\mu^u \sqrt{\frac{V}{r}}.$$

3 THE EINSTEIN FIELD EQUATIONS

Inside matter the Einstein tensor, calculated from (8), reads

$$G_{uu} = \frac{V_0 - 2\beta_0 V}{r^2} + \frac{V}{r^2}(e^{2\beta} - V_1 + 2\beta_1 V), \tag{16}$$

$$G_{ur} = \frac{1}{r^2}(e^{2\beta} - V_1 + 2\beta_1 V), \tag{17}$$

$$G_{rr} = \frac{4\beta_1}{r}, \tag{18}$$

$$G_\theta^\theta = G_\phi^\phi = e^{2\beta}\left\{2\beta_{01} - \frac{1}{2r^2}[rV_{11} - 2\beta_1 V + 2r(\beta_{11}V + \beta_1 V_1)]\right\}. \tag{19}$$

Outside matter we use Vaidya's metric; the only non-vanishing component of the Einstein tensor is

$$G_{uu} = -\frac{2\tilde{m}_0}{r^2}.$$

By substitution of (9) into (16)–(19) and use of the stress-energy tensor inside matter given by (12)–(15), the Einstein field equations, $G_{\mu\nu} = 8\pi T_{\mu\nu}$, can be written as

$$e^{-2\beta}\frac{r}{V}T_{uu} = \frac{1}{4\pi r(r-2\tilde{m})}[-\tilde{m}_0 e^{-2\beta} + (1-2\tilde{m}/r)\tilde{m}_1]$$

$$= \frac{1}{1-\omega^2}(\rho + 2\omega\mathscr{F} + P_r\omega^2), \tag{20}$$

$$e^{-2\beta}T_{ur} = \frac{\tilde{m}_1}{4\pi r^2} = \frac{1}{1+\omega}[\rho - \mathscr{F}(1-\omega) - P_r\omega], \tag{21}$$

$$e^{-2\beta}\frac{V}{r}T_{rr} = \beta_1\frac{r-2\tilde{m}}{2\pi r^2} = \frac{1-\omega}{1+\omega}(\rho - 2\mathscr{F} + P_r), \tag{22}$$

$$-T^\theta_\theta = -T^\phi_\phi$$

$$= -\frac{\beta_{01}e^{-2\beta}}{4\pi} + \frac{1}{8\pi}\left(1-2\frac{\tilde{m}}{r}\right)\left(2\beta_{11} + 4\beta_1^2 - \frac{\beta_1}{r}\right)$$

$$+ \frac{3\beta_1(1-2\tilde{m}_1) - \tilde{m}_{11}}{8\pi r} = P_\perp. \tag{23}$$

To solve algebraically four of the physical variables (ρ, P_r, $P_\perp$, ω and $\mathscr{F}$) from the above set of field equations (20)–(23), we must determine both β and $\tilde{m}$. We defer this to the next section. Here, however, we introduce some useful quantities for later use.

The mass function can be expressed as

$$\tilde{m} = \int_0^r 4\pi r^2 \tilde{\rho}\,dr. \tag{24}$$

It involves an effective energy density given by the right-hand side of (21),

$$\tilde{\rho} = \frac{1}{1+\omega}[\rho - \mathscr{F}(1-\omega) - P_r\omega], \tag{25}$$

which in the static limit reduces to the energy density of the system.

From (22) one has

$$\beta = \int_{a(u)}^r \frac{2\pi r^2}{r-2\tilde{m}}\frac{1-\omega}{1+\omega}(\rho - 2\mathscr{F} + P_r)\,dr,$$

and we may rewrite the non-static case as

$$\beta = \int_{a(u)}^r \frac{2\pi r^2}{r-2\tilde{m}}(\rho + \tilde{P})\,dr, \tag{26}$$

with

$$\tilde{P} = \frac{1}{1+\omega}[-\omega\rho - \mathscr{F}(1-\omega) + P_r] \tag{27}$$

being the effective pressure, which also reduces to the radial pressure in the static limit.

In principle, if β and $\tilde{m}$ were known, the four quantities, ρ, P_r, ω and $\mathscr{F}$ could be calculated from the field equations (20)–(23). Nevertheless, in the anisotropic case the appearance of the tangential pressure increases up to five the number of unknowns. To infer this relation from microphysical grounds would be desirable, but at present it is an extremely difficult task. Some authors (e.g. Herrera & Núñez 1990) approach the problem by assuming a particular hydrodynamic scenario: a homologous collapse (i.e. $\omega \propto r$). This may be regarded as a first-order approximation. This can be applied in the weak-field approximation only, and it has the drawback that to find higher order terms by this iterative method is a rather lengthy task. An alternative way is to introduce an additional equation. In the anisotropic static case, there can be found a general equation that relates the tangential pressure to the mass function, energy density and radial pressure. In the static case, the particular solution

$$P_\perp - P_r = \frac{1-h}{2}[\rho(r) + P(r)]\frac{m(r) + 4\pi r^3 P(r)}{r - 2m(r)},$$

where h is a parameter measuring the anisotropy, is the only one known for which the Einstein equations can be solved analytically (Cosenza et al. 1981). The range in which h takes values depends on the specific model. The isotropic case is recovered by letting $h = 1$. This expression is usually generalized to non-static cases by writing (Cosenza et al. 1982; Barreto & Rojas 1992)

$$P_\perp - P_r = \frac{1-h}{2}(\tilde{\rho} + \tilde{P})\frac{\tilde{m} + 4\pi r^3\tilde{P}}{r - 2\tilde{m}}. \tag{28}$$

In our case, the parameter h will be obtained, and the relation of the tangential versus radial stress evolves with the evolution of the sphere.

4 JUNCTION CONDITIONS AND SURFACE EQUATIONS

Matching the Vaidya metric to the Bondi metric at the surface ($r = a$) of the fluid distribution implies $\beta_a = \beta(u, r = a) = 0$, together with the continuity of the mass function $\tilde{m}(u, r)$ (i.e. the continuity of the first fundamental form). In addition, the continuity of the second fundamental form, $[K_{ij}]_{r=a} = K_{ij}|_{r=a+0} - K_{ij}|_{r=a-0} = 0$, leads to

$$-\beta_{0_a} + \left(1-2\frac{\tilde{m}_a}{a}\right)\beta_{1_a} - \frac{\tilde{m}_{1_a}}{2a} = 0 \tag{29}$$

(see Herrera & Jiménez 1983 for details).

Expanding β near $r = a(u)$ and restricting ourselves to the first order, we may write

$$\beta_{0_a} + \dot{a}\beta_{1_a} = 0, \tag{30}$$

where an overdot means d/du. Using (30) into (29), together with (24), (25) and (26), it follows that

$$\dot{a} = -\left(1-2\frac{\tilde{m}_a}{a}\right)\frac{\tilde{P}_a}{\tilde{P}_a + \tilde{\rho}_a}. \tag{31}$$

From the coordinate transformation (10), the velocity of matter in Bondi coordinates can be written as

$$\frac{dr}{du} = \frac{V}{r}\frac{\omega}{1-\omega},$$

and evaluated at the surface

$$\dot{a} = \left(1 - 2\frac{\tilde{m}_a}{a}\right)\frac{\omega_a}{1-\omega_a}. \qquad (32)$$

Comparing this expression with (31), it follows that

$$\check{P}_a = -\omega_a\tilde{\rho}_a, \qquad (33)$$

or equivalently using (25) and (27), we obtain

$$\mathcal{F}_a = P_{r_a}, \qquad (34)$$

which is a well-known result for radiative spheres (Santos 1985).

To derive the surface equations, we introduce five dimensionless functions,

$$A \equiv \frac{a}{m(0)} \quad M \equiv \frac{m}{m(0)} \quad u \equiv \frac{u}{m(0)} \quad F \equiv 1 - \frac{2M}{A} \quad \Omega \equiv \frac{1}{1-\omega_a}, \qquad (35)$$

where $m(0)$ is the initial mass of the system. Using in (32) the functions just defined, we obtain the first surface equation,

$$\dot{A} = F(\Omega - 1). \qquad (36)$$

The second surface equation emerges from the luminosity evaluated at the surface of the system. The luminosity, as seen by a comoving observer, is defined as

$$\hat{E} = (4\pi r^2\mathcal{F})_{r=a}.$$

Evaluating (20) and (21) at the surface, and using the expansion

$$\tilde{m}_{0_a} \approx \dot{\tilde{m}} - \dot{a}\tilde{m}_{1_a}, \qquad (37)$$

the luminosity perceived by an observer at rest at infinity reads

$$L = -\dot{M} = \hat{E}(2\Omega - 1)F. \qquad (38)$$

The function F is related to the boundary redshift z_a by

$$1 + z_a = \frac{\nu_{em}}{\nu_{rec}} = F^{-1/2}.$$

Thus the luminosity as measured by a non-comoving observer located on the surface is

$$E = L(1+z_a)^2 = -\frac{\dot{M}}{F} = \hat{E}(2\Omega - 1),$$

where the term $(2\Omega - 1)$ accounts for the boundary Doppler-shift. Using relationship (38) together with the first surface equation, we obtain the second surface equation,

$$\dot{F} = \frac{2L + F(1-F)(\Omega - 1)}{A}. \qquad (39)$$

The third surface equation is model-dependent. For anisotropic fluids, the relationship $(T^\mu_{r;\mu})_a = 0$ can be written as

$$-\left(\frac{\check{P}+\tilde{\rho}}{1-2\tilde{m}/r}\right)_{0_a} + \tilde{R}_{\perp_a} - \left[\frac{2}{r}(P_r - \check{P})\right]_a = 0, \qquad (40)$$

where

$$\tilde{R}_{\perp_a} = \check{P}_{1_a} + \left(\frac{\check{P}+\tilde{\rho}}{1-2\tilde{m}/r}\right)_a \left(4\pi r\check{P} + \frac{\tilde{m}}{r^2}\right)_a - \left[\frac{2}{r}(P_\perp - P_r)\right]_a.$$

Using the expansions (37) and

$$(\tilde{\rho}+\check{P})_{0_a} \approx [\tilde{\rho}_a(1-\omega_a)]_0 - \dot{a}(\check{P}+\tilde{\rho})_{1_a},$$

where (33) has been used, we obtain, after a straightforward calculation,

$$\frac{\dot{F}}{F} + \frac{\dot{\Omega}}{\Omega} - \frac{\dot{\tilde{\rho}}_a}{\tilde{\rho}_a} + F\Omega^2\frac{\tilde{R}_{\perp_a}}{\tilde{\rho}_a} - \frac{2}{A}F\Omega\frac{P_{r_a}}{\tilde{\rho}_a} = G(F, \Omega, A), \qquad (41)$$

where

$$G(F, \Omega, A) = (1-\Omega)\left[4\pi A\tilde{\rho}_a\frac{3\Omega-1}{\Omega} - \frac{3+F}{2A} + F\Omega\frac{\tilde{\rho}_{1_a}}{\tilde{\rho}_a} + \frac{2F\Omega}{A\tilde{\rho}_a}(P_\perp - P_r)_a\right].$$

The first surface equation (36) gives the evolution of the radius of the star. The second one relates the total mass-loss rate to the energy flow through the surface, and expresses the evolution of the redshift at the surface. Expression (40), or, equivalently the third surface equation (41), is the generalization of the Tolman–Oppenheimer–Volkov equation to the non-static radiative anisotropic situation.

The algorithm of the HJR method as applied to this model may be summarized as follows.

(i) Take a static, but otherwise arbitrary, interior solution of the Einstein equations for a spherically symmetric fluid distribution,

$$P_{st} = P(r), \qquad \rho_{st} = \rho(r).$$

(ii) Assume

$$\tilde{\rho} \equiv \tilde{\rho}(u, r),$$

$$\check{P} \equiv \check{P}(u, r),$$

and that in the static limit these functions reduce to ρ_{st} and P_{st}, respectively. The junction condition (33) relates the time-dependence of both quantities.

(iii) Introduce $\tilde{\rho}(u, r)$ and $\check{P}(u, r)$ into (24) and (26) to determine $\tilde{m}$ and β up to three unknown functions of time.

(iv) Obtain these three functions of u by solving a system of ordinary differential equations evaluated at the surface. The first two, which come from (36) and (39) respectively, do not depend on the choice of the static interior solution; however, the third one, which arises from

$$(T^\mu_{1;\mu})_a = 0,$$

does not enjoy such a property.

(v) Impose one of the four unknown functions – A, F, Ω or L. Usually the function L related to the luminosity is chosen, as it is an observational parameter.

(vi) Once these three functions are known, determine $\tilde{m}$ and β. After this, the Einstein equations (20)–(23), supplemented by (28), constitute a closed system of differential equations.

The rationale behind the assumption on the r-dependence of the *effective variables* $\check{P}$ and $\tilde{\rho}$ [points (i) and (ii) of the above method] can be grasped in terms of the characteristic times for different processes involved in a collapse scenario. If the hydrostatic time-scale $\mathscr{T}_{\text{HYDR}}$, which is of the order $\sim 1/\sqrt{G\rho}$ (where G is the gravitational constant, and ρ denotes the mean density), is much smaller than the Kelvin–Helmholtz time-scale $\mathscr{T}_{\text{KH}}$, then in a first approximation the inertial terms in the equation of motion (41) can be ignored (Kippenhahn & Weigert 1990). Therefore in this first approximation the r-dependence of P and ρ is the same as in the static solution. Then the assumption that the *effective variables* (21) and (27) have the same r-dependence as the physical variables of the static situation represents a correction to that approximation, and is expected to yield good results whenever $\mathscr{T}_{\text{KH}} \gg \mathscr{T}_{\text{HYDR}}$. Fortunately, $\mathscr{T}_{\text{KH}} \gg \mathscr{T}_{\text{HYDR}}$ for almost all kinds of stellar objects. Thus, for example, for the Sun we get $\mathscr{T}_{\text{KH}} \sim 10^7$ yr, whereas $\mathscr{T}_{\text{HYDR}} \sim 27$ min. Also, the Kelvin–Helmholtz phase of the birth of a neutron star lasts for about tens of seconds (Burrows & Lattimer 1986), whereas for a neutron star of one solar mass and a 10-km radius, we obtain $\mathscr{T}_{\text{HYDR}} \sim 8.61 \times 10^{-11}$ s.

5   THE MODEL

5.1   The radiation scenario: a differentiated anisotropic layer model

Our aim is to describe the gravitational collapse of a dense star composed by a mixture of radiation and viscous matter. Depending on the degree of interaction between both components, we may speak of three differentiated zones.

(1) The *core*. The evolution of this inner zone is governed by the diffusion process. Matter and radiation interact strongly, and so they have the same temperature within this region. In the core of the star, the opacity of the collapsing matter enhances the diffusion process (Kazanas 1978).

(2) The *transition zone*. Along this region the system undergoes the transition from the diffusion approximation (DA) to the free streaming-out limit (FL).

(3) The *crust*. This zone is limited to a thin layer which comprises the most external part of the star; in it the radiation practically does not interact with matter, and the viscous stresses vanish.

We assume that in the crust the free streaming-out limit prevails. Since viscous processes arise from interaction between matter and radiation, they must vanish there. It is therefore possible to determine the tangential pressure at the surface. Evaluating equation (6) at $r = a$, and using (34), we obtain

$$P_{\perp a} = \mathscr{F}_a + \tfrac{1}{2}(\rho_r - 3\mathscr{P}).$$

In the free streaming-out limit the condition $\rho_r = \mathscr{P} = \mathscr{F}$ is obeyed; thus last expression implies

$$P_{\perp a} = 0. \tag{42}$$

Likewise, inspection of (5) reveals that the material pressure also vanishes at the surface.

The vanishing of the viscosity coefficients at the surface imposes a time-dependence on the anisotropy parameter h. This differs from the anisotropic diffusive case in which h is taken as a constant. Evaluating expression (28) at the surface, and using (38) and condition (33), h can be expressed as

$$h = 1 + \frac{L\Omega^2}{\pi A^2 (2\Omega - 1)[(1 - F)\Omega - 8\pi A^2 (\Omega - 1)\tilde{\rho}_a]\tilde{\rho}_a}. \tag{43}$$

From the dependence on L and Ω of this expression, we may conclude that the rate of total mass loss and the velocity of the surface strongly affect the deviation of the system from isotropy. In fact, a non-radiating configuration should be isotropic. This contrasts with some previous non-viscous models where the luminosity has been found to be independent of the anisotropy of the fluid (Chan 1993).

It is clear that, in order to describe the evolution of the radiation through the matter configuration, the relativistic radiation transfer equation (see Anile & Romano 1994 and Nobili, Turolla & Zampieri 1993, and other recent references therein) should be solved together with the Einstein equations, provided that the junction conditions are satisfied. In this way the above radiation moments 1, 2 and 3 are related to the physical properties of the medium (absorption and/or emission) and to the geometry of the space–time. However, this lies far beyond the purpose of the present work. Despite this, it is possible to consider several other physically interesting situations in the above-mentioned limits (i.e. *free streaming-out* and *diffusion*) and the physical scenario described above.

5.2   Evolution of the Schwarzschild anisotropic viscous solution

We consider a solution inspired by the homogeneous Schwarzschild anisotropic interior solution (Cosenza et al. 1981). In this model, the energy density and the radial and tangential pressures are given in the static case by

$$\rho = \rho_o,$$

where ρ_o is a constant,

$$P_r = \rho\left[\frac{(1 - (8\pi/3) r^2 \rho)^{h/2} - (1 - (8\pi/3) a^2 \rho)^{h/2}}{3(1 - (8\pi/3) a^2 \rho)^{h/2} - (1 - (8\pi/3) r^2 \rho)^{h/2}}\right],$$

and

$$P_\perp - P_r = \frac{1 - h}{2}(\rho + P_r)\left(\frac{m(r) + 4\pi r^3 P_r}{r - 2m(r)}\right),$$

respectively. The homogeneous Bethe–Borner–Sato (BBS) equation of state is largely accepted for 'Newtonian' neutron stars (Borner 1973; Shapiro & Teukolsky 1983; Demiański 1985; Kippenhahn & Weigert 1990). It presents an energy density practically constant along the system, except at the surface where it decreases abruptly. The static Schwarzschild model is, among all known relativistic solutions of the Oppenheimer–Volkov equation, closer to the BBS equation of state, but it cannot resemble the abrupt vanishing of the energy density because of the junction conditions. The imposition in our model of a free streaming-out limit at the surface (the *crust*) is an attempt to mimic the behaviour of the BBS

equation of state, although the Schwarzschild solution cannot do it. Besides, this homogeneous solution represents, in the static limit, an incompressible fluid of constant density. Despite its simplicity, this equation of state is not deprived of some additional physical interest. The homogeneity of the mass energy density in this model enables us to study the viscous hydrodynamic effects on radiating spheres in General Relativity under conditions that are 'more extreme' than any available with 'more normal' physical equations of state.

Following the HJR method, outlined above, as applied previously to the anisotropic diffusive case (Cosenza et al. 1982; Barreto & Rojas 1992), we generalize these expressions to

$$\tilde{\rho} = \begin{cases} (3/8\pi) f(u), & \text{if } r \le a(u), \\ 0 & \text{otherwise,} \end{cases} \tag{44}$$

$$\tilde{P}_r = \frac{3f(u)}{8\pi} \left\{ \frac{g(u)[1-f(u) r^2]^{h/2} - [1-f(u) a^2]^{h/2}}{3[1-f(u) a^2]^{h/2} - g(u)[1-f(u) r^2]^{h/2}} \right\}, \tag{45}$$

where, via (33), the auxiliary function $g(u)$ is found to be

$$g(u) = \frac{1 - 3\omega_a}{1 - \omega_a},$$

and

$$P_\perp - P_r = \frac{1 - h(u)}{2} (\tilde{\rho} + \tilde{P}) \left[\frac{\tilde{m}(u, r) + 4\pi r^3 \tilde{P}}{r - 2\tilde{m}(u, r)} \right]. \tag{46}$$

Note that equation (44) is a consequence of points (i) and (ii) of the HJR method. By substitution of (44) into (24), it follows that

$$\tilde{m} = \begin{cases} (r^3/2) f(u), & \text{if } r < a(u), \\ (a^3/2) f(u) & \text{if } r \ge a(u). \end{cases}$$

Using the expressions (44) and (45) in (26), it follows that

$$\beta = \frac{1}{2h} \ln \left[(1 - \omega_a) \left(\frac{3(1 - fa^2)^{h/2}}{2(1 - fr^2)^{h/2}} - \frac{1}{2} \right) + \omega_a \right], \quad \text{if } r < a(u),$$

$\beta = 0$ otherwise. By resorting to (35), the three unknown functions of u (i.e. f, a and ω_a) can be written in terms of F, A and Ω. Thus the system of three differential equations reads

$$\dot{A} = F(\Omega - 1), \tag{47}$$

$$\dot{F} = \frac{1}{A} [2L + F(1 - F)(\Omega - 1)], \tag{48}$$

$$\dot{\Omega} = -\frac{\dot{F}\Omega}{F(1 - F)} - \frac{(1 - F)}{2A} [(2 + h)\Omega(2\Omega - 3) + 3], \tag{49}$$

where expressions (41), (44) and (45), and condition (42) were used. From (43) and (44), the anisotropy parameter can be written as

$$h = 1 + \frac{8L}{3(2\Omega - 1)(1 - F)^2(3 - 2\Omega)}.$$

To close the system of equations, we suppose that the loss of mass of the sphere can be described by a Gaussian pulse centred at $u = u_0$,

$$-\dot{M} = L = \frac{M_{\text{rad}}}{\lambda\sqrt{2\pi}} e^{(1/2)[(u - u_0)/\lambda]^{1/2}}, \tag{50}$$

where λ is the width of the pulse, and M_{rad} is the total mass lost in the process.

Now we are in a position to integrate the system of three surface equations (47), (48) and (49) for an arbitrary initial set of data, and to determine β and $\tilde{m}$. Then the four field equations (20)–(23) can be numerically solved, and four physical quantities can be found, for instance ω, $\mathscr{F}$, ρ and P_r. The tangential pressure follows from (46).

We select the following set of initial data,

$$A(0) = 10, \qquad F(0) = 0.8, \qquad \Omega(0) = 1,$$

which corresponds to a dense star initially at rest. In the HJR approach, models are restricted only by several minimum reasonable physical requirements:

$$\rho(r, u) > 0, \qquad \rho(r, u) > P(u, r), \qquad \tilde{m}(r, u) < \tfrac{1}{2} r,$$
$$-1 < \omega(r, u) < 1. \tag{51}$$

Consequently, these requisites suggest the running time for performing simulations.

The figures we describe (Figs 1–16) correspond to the physical variables of a model with a total radiated energy taken as a 20 per cent of the initial mass. The hydrodynamic outcome (compression wave and the double peak in the radiation energy flow density) is also present in simulations with less radiated mass (i.e. 10, 5, 1 and 0.5 per cent of the initial mass), but we have a crisper effect with the selected model. In addition, these results do not differ qualitatively from the corresponding ones for the non-static $\Omega(0) < 1$ initial configurations.
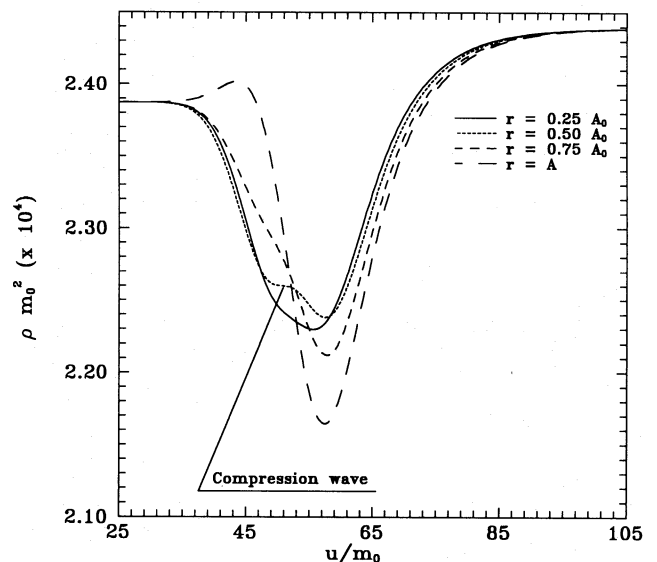

Figure 1. Dimensionless energy density as a function of the dimensionless time-like coordinate. Notice the effect of the compression wave in the inner shells.
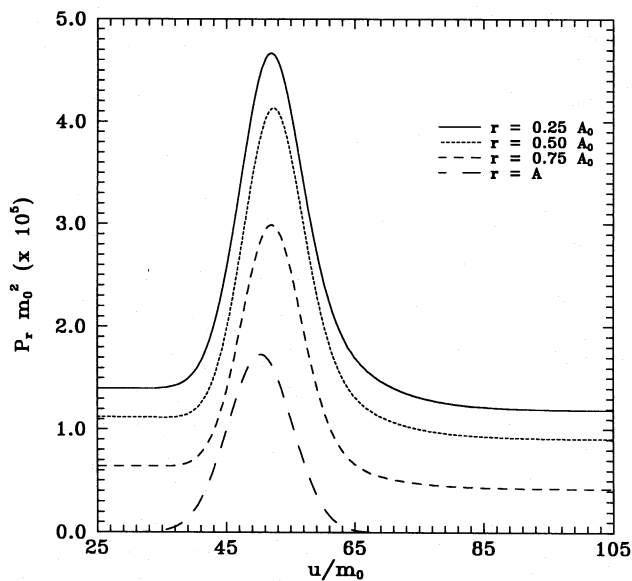
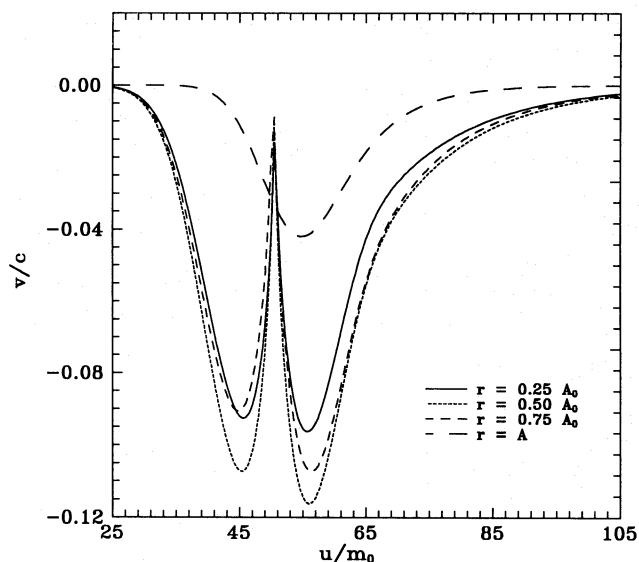**Figure 2.** Evolution of the dimensionless radial pressure.
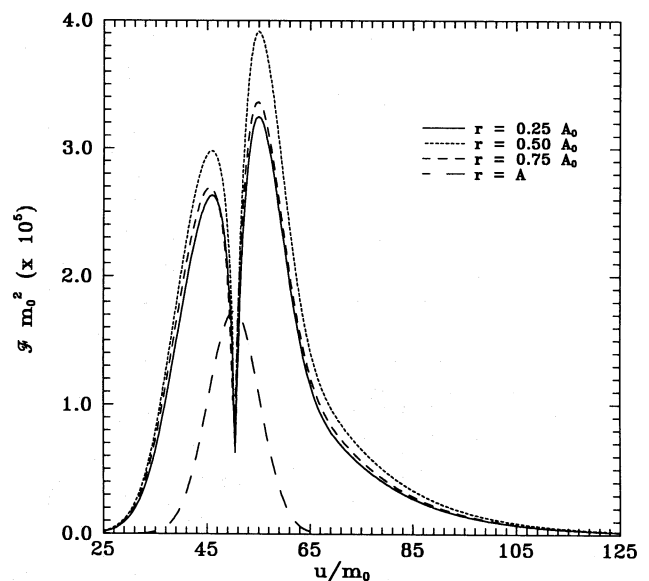

Figure 4. Dimensionless radiation energy density flow as a function of the time-like coordinate. The elapsed time between equilibrium states, i.e. when $\mathscr{F}$ can be neglected in the core, is about $\Delta(u/m_0) \approx 100$.
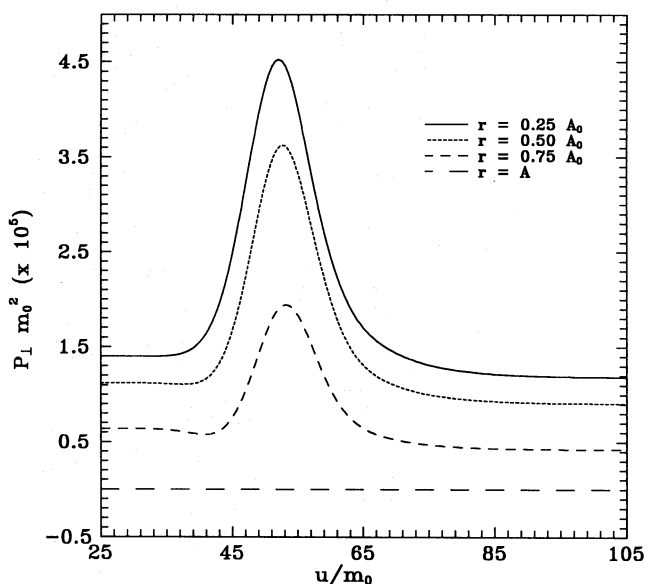

Figure 3. Evolution of the matter velocity in Bondi coordinates $(\mathrm{d}r/\mathrm{d}u)$.

Figure 5. Evolution of the dimensionless tangential pressure. Note that it vanishes at the surface.

5.3 Viscosity and radiation

The transport coefficients of a radiating fluid with mean free time τ are given in the diffusion approximation by Weinberg (1971),

$$\eta_{\mathrm{DA}} = \frac{4}{15}\,\alpha\rho_r\tau,$$

$$\zeta_{\mathrm{DA}} = 15\eta_{\mathrm{DA}}\left[\frac{1}{3} - \left(\frac{\partial P}{\partial\rho}\right)_n\right]^2, \qquad (52)$$

$$\chi = \frac{4}{3}\,\alpha\tau\frac{\rho_r}{T},$$

where η_{DA} and ζ_{DA} are the shear and bulk viscosity coefficients in the diffusion approximation, χ is the thermal conductivity coefficient, and α is a constant parameter that takes the values 1 and 7/8 for photons and neutrinos, respectively.

In radiation hydrodynamics it is customary (Mihalas & Mihalas 1984) to introduce two useful quantities, the Eddington factors, defined by

$$r_1 = \frac{\mathscr{F}}{\rho_r}, \qquad r_2 = \frac{\mathscr{P}}{\rho_r}. \qquad (53)$$
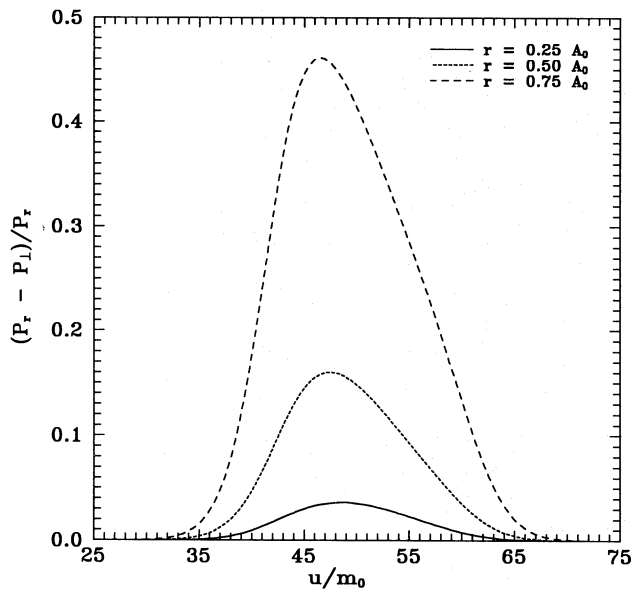
Figure 6. Normalized anisotropy as a function of the dimensionless time-like coordinate. It increases with the distance to the centre.
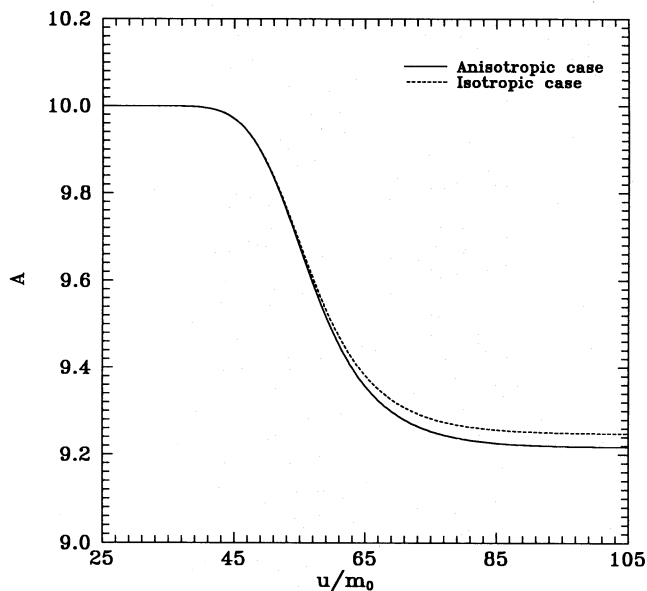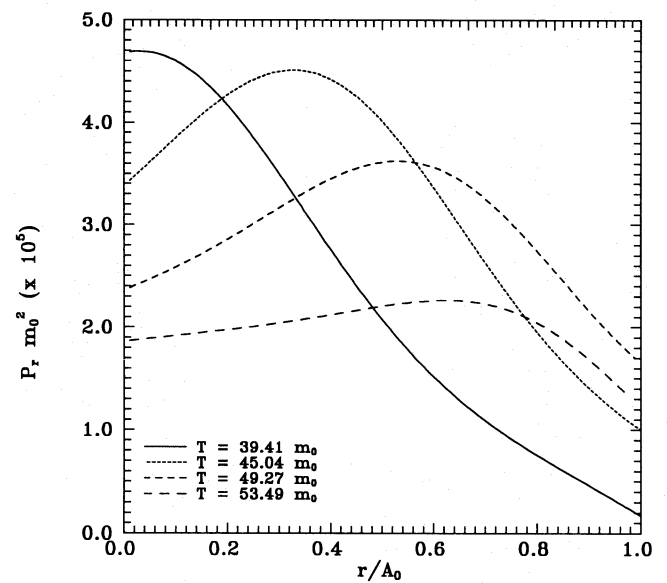

Figure 8. Dimensionless radial pressure as a function of the radial coordinate. The curves are constructed using equation (11) at constant Schwarzschild time T.
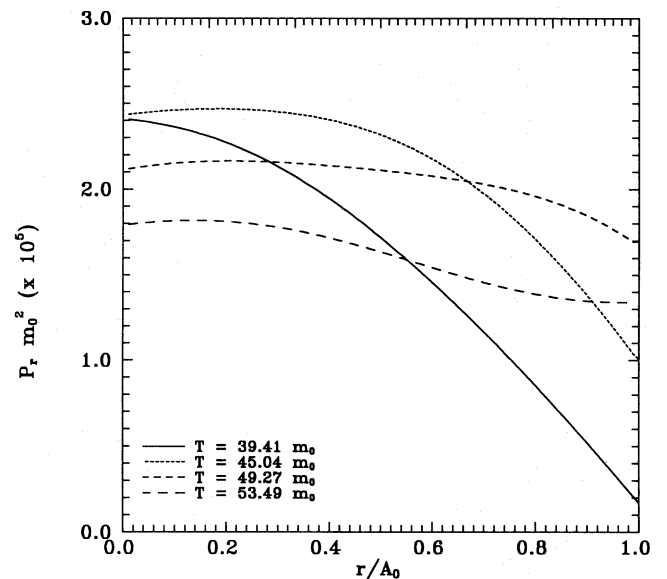

Figure 7. Evolution of the radius of the star.

Figure 9. Dimensionless radial pressure as a function of the radial coordinate in the isotropic case. The curves are constructed as in Fig. 8.

The first one, r_1, measures the deviation of the system from DA, whereas r_2 establishes a sort of 'state equation' for the radiation. The first factor lies within the range

$$0 \leq r_1 \leq 1,$$

the lower value corresponding to the equililibrium situation, and the upper one to free streaming. In DA the value of r_1 can be taken as 1/3 (Mihalas & Mihalas 1984). Therefore, in the non-equilibrium state, it may vary within

$$r_1^{DA} = \tfrac{1}{3} \leq r_1 \leq 1 = r_1^{FL}.$$

From (6), we infer that the deviation of the system from DA is also measured by the difference between the tangential and
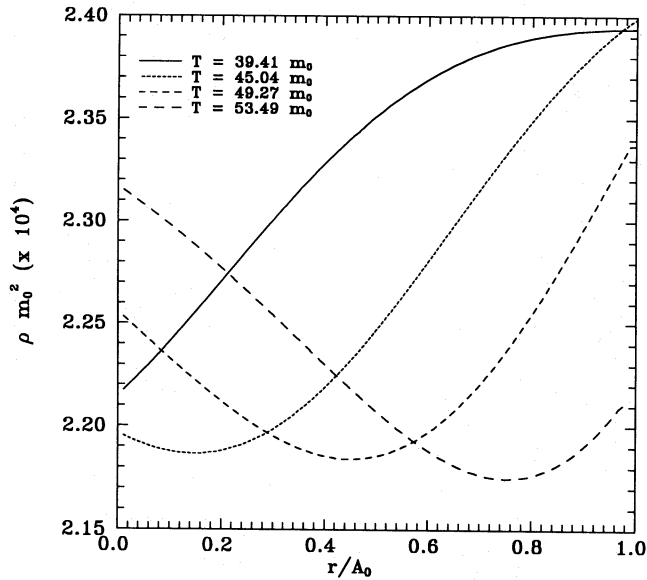
radial pressures. Accordingly, we introduce a new parameter which accounts for the relative anisotropy of the system,

$$\Delta = \frac{P_r - P_\perp}{P_r} .$$

It can be related to the optical depth, and it seems reasonable to suppose that both quantities – Δ and r_1 – are connected, although there are some limitations to the form in which both parameters can be related. An inspection of Fig. 6 reveals that this parameter in our modelling lies within the range
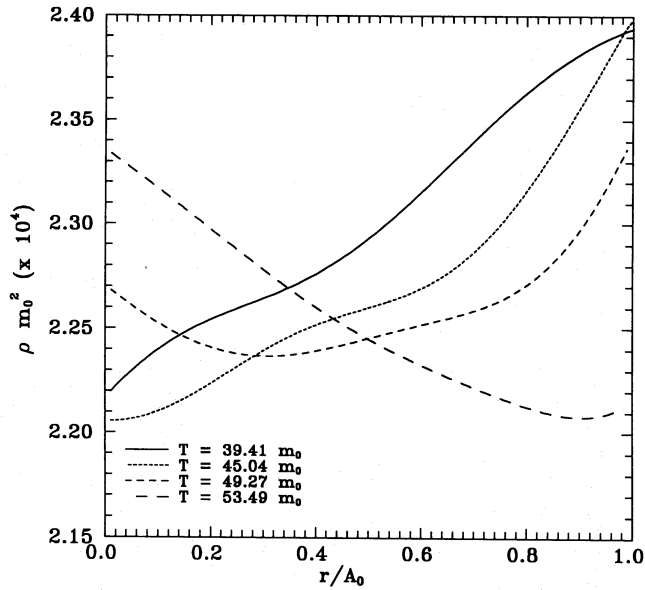
Figure 10. Dimensionless energy density in the anisotropic case. The curves are constructed as in Fig. 8.
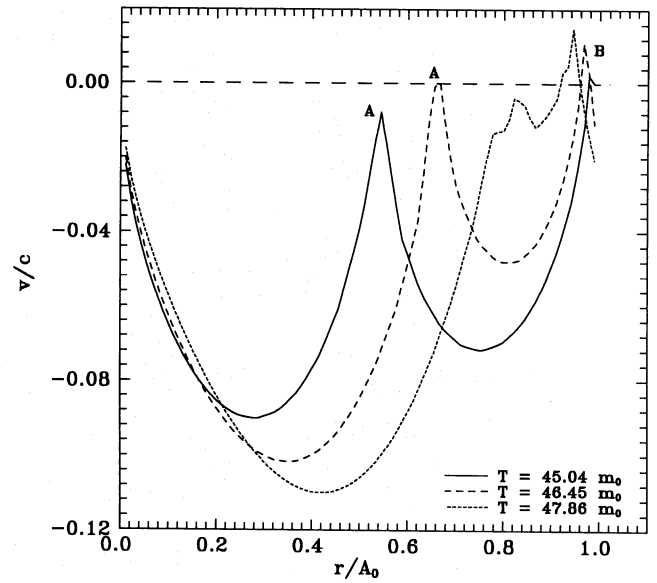

Figure 11. Same as Fig. 10 for the isotropic case.

Figure 12. Matter velocity in Bondi coordinates for different values of Schwarzschild time *T*. Points marked A are affected by the compression wave, and points marked B by the sudden increase of the stiffness of the material.
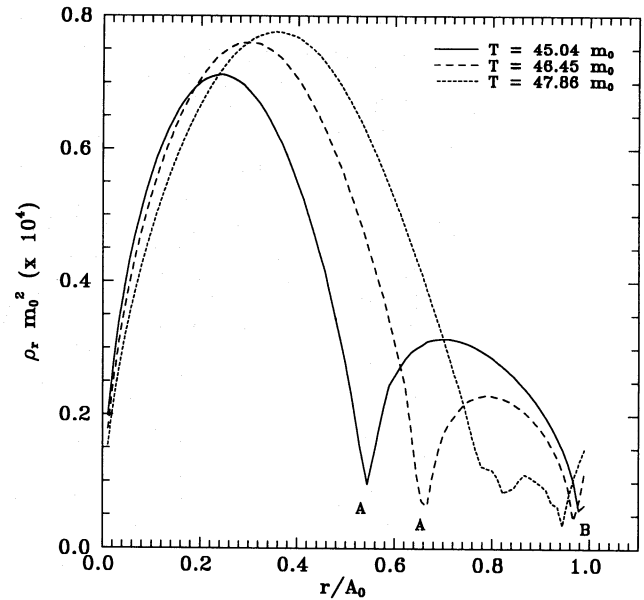
Figure 13. Dimensionless radiation energy density as a function of the radial coordinate. Points marked either A or B have the same meaning as in Fig. 12.

$0 \leq \Delta \leq 1$. The isotropic condition is fulfilled in the centre, where Δ vanishes. In this case, the first Eddington factor reduces to r_1^{DA}. On the other hand, Δ reaches its maximum value at the surface, where $P_\perp$ vanishes and $r_1 = r_1^{FL}$. Consequently, for our matter distribution it seems that the simplest way to comply with these requirements is to assume that

$$r_1 = r_1^{DA} + (r_1^{FL} - r_1^{DA}) \Delta. \tag{54}$$

In addition to the simplicity of this interpolation, the influence of the energy radiation flow on the anisotropy of the medium is clear.

As mentioned above, the viscous coefficients vanish in the free streaming limit, i.e. in our case in the crust. In the core,

where the diffusion approximation holds, the viscosity coefficients are simply given by (52). Although their behaviour in the transition zone is unknown, they are bound to vary continuously from the core to the crust. We may model their behaviour in the transition zone with the help of a weight function, $f(r_1)$. For simplicity, we take this as

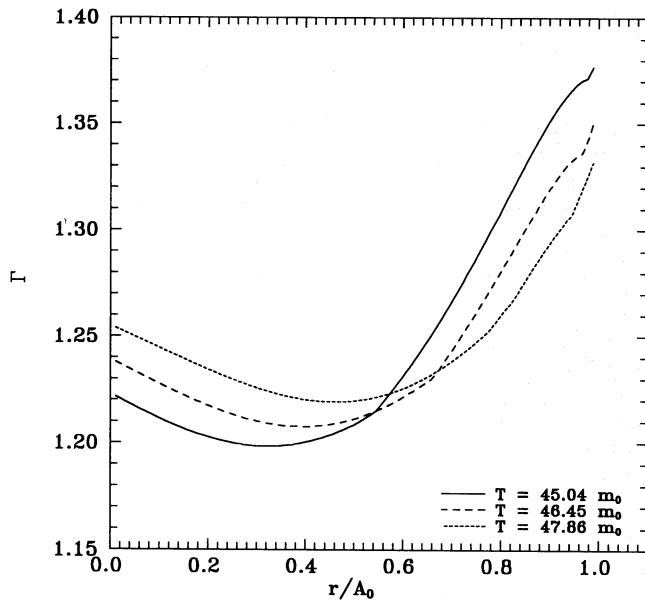$$f(r_1) = \frac{r_1^{FL} - r_1}{r_1^{FL} - r_1^{DA}}.$$

Figure 14. Coefficient Γ, defined in equation (55), as a function of the radial coordinate. Note the behaviour close to $r = A_0$.
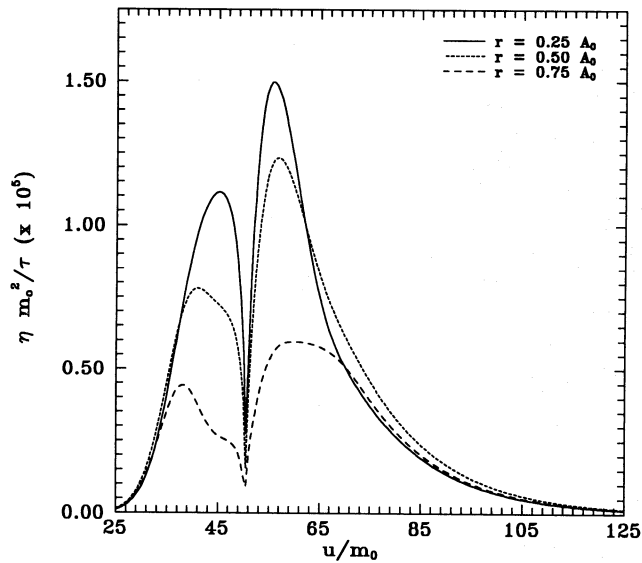
Figure 16. Evolution of the bulk viscosity coefficient.

5.4 Compressibility index for radiating fluids

In order to understand further the picture emerging from our modelling, use has been made of a generalization of the concept of compressibility index for non-adiabatic systems. For radiating bodies the adiabatic index

$$\Gamma = \frac{\mathrm{d}\ln P}{\mathrm{d}\ln \rho}$$

does not faithfully measure the stiffness of the system since, in addition to the hydrodynamic pressure, other sources contribute to the flow of momentum. Following Barreto et al. (1992), we define

$$\Gamma = \frac{\mathrm{d}\ln \Pi}{\mathrm{d}\ln e}, \tag{55}$$

where

$$\Pi = \gamma^3[2\rho\omega^2 + P_\mathrm{r}(1+\omega^2) + \omega\mathscr{F}(3+\omega^2)]$$

and

$$e = \gamma^2(\rho + P_\mathrm{r}\omega^2 + 2\mathscr{F}\omega)$$

are the total flow of momentum in the radial direction and the energy density measured by a locally Minkowskian observer, respectively.

Figure 15. Evolution of the shear viscosity coefficient.

Under this assumption, the viscous coefficients in the transition zone may be written as

$$\eta = f(r_1)\,\eta_\mathrm{DA},$$

$$\zeta = 15\eta\left[\frac{1}{3} - \left(\frac{\partial P}{\partial \rho}\right)_n\right]^2,$$

which complete the interplay among radiation flow, viscosity and anisotropy. Of course, the above strategy does not apply to the thermal conductivity coefficient, which is only defined for the diffusive regime. Now, from (54) and (53), the radiation energy density can be found and, for a given τ, the viscous coefficients follow.
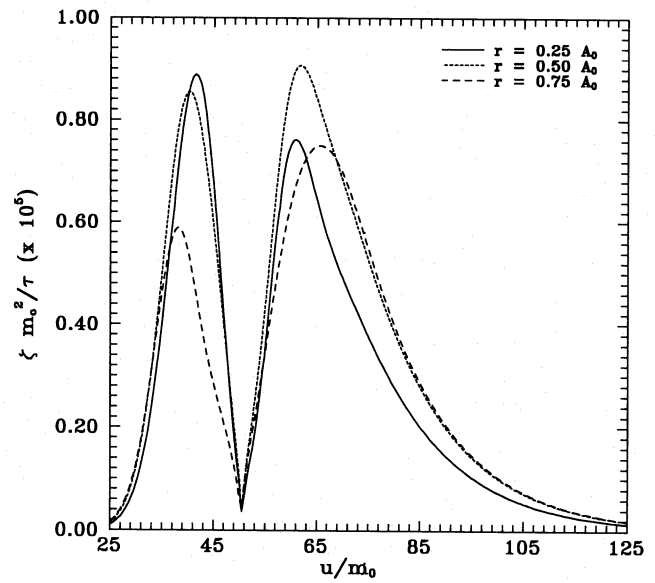
6 DISCUSSION

We are aware of the fact that the collapse of a 'real' massive star described as an interior solution of Einstein equations using a 'physical' nuclear equation of state with the corresponding opacities (and emissivities) for the emerging radiation (photons and neutrinos) and fluid material stresses is far from solved. Our main concern in this paper has been to explore the hydrodynamic consequences of solving the Einstein equations for a bounded (fully matched interior with

the exterior solution) spherical distribution of matter where viscous and radiation effects could be relevant. In order to solve the Einstein system of equations, several heuristic assumptions have been adopted concerning the radiation scenario and the nuclear equation of state for the matter distribution. These assumptions seem to be reasonable, and they describe a plausible general relativistic gravitational collapse.

Using the above-mentioned method, we have been able to work out the physical variables of a model which is free of singularities everywhere, matched with the exterior Vaidya metric. There are two processes that may induce anisotropy in the system, namely the shear viscosity and the non-diffusive radiation. As mentioned above, as long as the non-diffusive radiation dominates in the external layers, the viscous pressure in the crust is negligible. In the core, however, the situation is quite different, as the shear viscosity predominates there. As can be seen in Fig. 6, the anisotropy increases with the distance from the centre of the star, which shows that the largest contribution to the anisotropy is due to the non-diffusive radiation. By contrast, the contribution of the shear viscosity, which is important in the core, is much lower. In the initial stages the radiative transfer in the star is dominated, except in the crust, by diffusion process; later, during the collapse, the system approaches free streaming. Nevertheless, the radiation in the core remains close to DA.

In order to evaluate the differences between anisotropic and isotropic cases, we have integrated the system of three differential equations in the isotropic case. This model is recovered from the anisotropic one by taking $h = 1$ and setting viscous coefficients to zero everywhere. Except at the surface, the different behaviour of these two models becomes manifest throughout the star, since the loss of mass is given by (50) with the same values for λ, M_{rad} and u_0.

Initially the energy density, as in the Schwarzschild model, is constant throughout the star. The collapse starts when an instability is produced in the centre. Then the central energy density decreases, and the condition $\partial \rho / \partial r \leq 0$ ceases to be fulfilled. This instability propagates throughout the star and eventually reaches the surface which falls down. Then the energy density starts growing in the centre, and the system evolves toward equilibrium.

Although the loss of mass is the same in both cases, the radius of the star in the new equilibrium state is larger in the isotropic case (Fig. 7); hence the compact objects produced in anisotropic collapses are denser and stiffer. This property seems to be independent of the radiating anisotropic model adopted (Chan 1993).

The pressure in the centre mounts up to a maximum value and decreases immediately thereafter. This variation of the central pressure generates a compression wave which travels to the surface (Figs 8 and 9). Its maximum value in the anisotropic case is roughly double that of the isotropic one and, consequently, the dynamics of the system are much more influenced by the compression wave in this case. Since in the isotropic case the wave is comparatively weak, the energy density remains nearly unaffected. By contrast, in the anisotropic collapse the wave is much stronger, and consequently the variations in the energy density are seriously inhibited – compare Figs 10 and 11. It can safely be said that in the latter case the star becomes stiffer. On its way towards the surface the compression wave becomes so attenuated that it

vanishes at $r \approx 0.7 A_0$ (Fig. 8). At the same time as the mass loss is reduced, and consequently the luminosity, the compression wave becomes weak and, as mentioned above, the system comes close to the isotropic case.

Because of the presence of viscous processes, the interior radiation energy density flow is, in the anisotropic case, larger than it is in the isotropic case. When any spherical shell is traversed by the compression wave, the pressure gradient changes its sign in it. Thus this diminishes its radial velocity, and the radiation energy density flow and radiation energy density decrease accordingly – Figs 12 and 13. Once the compression wave has gone through it, it increases its radial velocity towards the centre and the radiation energy density flow augments. In our opinion, this is the origin of the formation of two successive maxima in the radiation energy density flow in the shell (Fig. 4). The compression wave cannot account for the behaviour observed just beneath the surface. In these external layers a minimum in the radiation energy density flow and in the radiation energy density (Fig. 13) is transmitted from the surface to the interior. To clarify this surface effect, we resort to the concept of compressibility.

The resistance of the shells close to the surface to being compressed increases abruptly (Fig. 14). This effect only affects a few shells close to the surface, and it is transmitted inwards. Consequently, the matter close to the surface reverses its velocity and starts to travel outwards (Fig.12).

The width of the pulse imposed over M is very small. Thus, for $m(0) = 1\,M_\odot$, the time elapsed between the equilibrium states is shorter than 1 ms. The core reaches equilibrium only about 0.50 ms after the beginning of the collapse (Fig. 4). When the collapse lasts for about 1 s, the behaviour of the system is very simple; all variations in pressure and energy density have plenty of time to get through the sphere before the collapse ends. As a consequence, the process is quasi-static, and the hydrodynamic collapse time-scale is of the order of magnitude of the diffusion time-scale.

Since the system of differential equations (47)–(49) is evaluated at the surface, our assumption of three different layers does not affect their solution. This model may be justified a posteriori as follows. When the collapse is very fast, the hydrodynamic collapse time-scale is about 0.50 ms (Fig. 4). If the free streaming-out limit were valid throughout the star, the radiation generated in the centre would reach, for an initial radius about 15 km, the surface in approximately 0.05 ms. This indicates that the radiation finds some obstacle on its way outwards. Furthermore, viscosity stresses are present only in the diffusion approximation zones, and some of the effects seen in the inner core seem inexplicable beyond this limit.

The radiation energy density allows us to find an upper bound to the speed of the collapse. Because the material part is positive-definite, the relationship

$$\rho_M = \rho - \rho_r > 0$$

holds. The radiation energy density is obtained from (53), and increases with the radiation energy density flow. Both the total loss of mass in the collapse M_{rad} and the width of the pulse λ are input data in the model. If M_{rad} is increased or λ decreased, the radiation energy density flow increases, and for some values of M_{rad} and λ the radiation energy density

outweighs the total energy density. Hence these sets of values must be discarded.

As can be seen by contrasting Figs 15 and 16, the behaviour and order of magnitude of both viscosity coefficients are similar. Thus, for a mixture of matter and radiation, the bulk viscosity should not be neglected in favour of the shear viscosity a priori.

ACKNOWLEDGMENTS

REFERENCES

Aguirre F., Hernández H., Núñez L. A., 1994, Ap&SS, in press
Anile A. M., Romano V., 1992, ApJ, 386, 325
Aquilano R., Barreto W., Núñez L. A., 1994, Gen. Relativ. Gravitation, in press
Bahcall J. N., 1989, Neutrino Astrophysics. Cambridge Univ. Press, Cambridge
Barreto W., Núñez L. A., 1991, Ap&SS, 178, 261
Barreto W., Rojas S., 1992, Ap&SS, 193, 201
Barreto W., Herrera L., Santos N., 1992, Ap&SS, 187, 271
Bondi H., 1964, Proc. R. Soc. London, A281, 39
Bondi H., Van der Burg, M. G. J., Metzner A. W. K., 1962, Proc. R Soc. London, A269, 21
Borner G., 1973, On the Properties of Matter in Neutron Stars. Springer Tracts in Physics, Springer, Berlin
Bruenn S. W., 1985, ApJS, 58, 771
Burrows A., Lattimer J. M., 1986, ApJ, 307, 178
Chan R., 1993, Ap&SS, 206, 219
Cosenza M., Herrera L., Esculpi M., Witten L., 1981, J. Math. Phys., 22, 118
Cosenza M., Herrera L., Esculpi M., Witten L., 1982, Phys. Rev. D, 25, 2527
Demiański M., 1985, in ter Haar D., ed., Relativistic Astrophysics, International Series in Natural Philosphy, Vol. 110. Pergamon Press, Oxford
Herrera L., Jiménez J., 1983, Phys. Rev. D, 28, 2987
Herrera L., Núñez L. A., 1990, Fundam. Cosmic Phys., 14, 235
Herrera L., Jiménez J., Ruggeri G., 1980, Phys. Rev. D, 22, 2305 (HJR)
Herrera L., Melfo A., Núñez L. A., Patiño A., 1994, ApJ, 421, 677
Kazanas D., 1978, ApJ, 222, L109
Kazanas D., Schramm D., 1979, in L. Smarr, ed., Sources of Gravitational Radiation. Cambridge Univ. Press, Cambridge, p. 345
Kippenhahn R., Weigert A., 1990, Stellar Structure and Evolution. Springer-Verlag, Berlin, p. 11
Lindquist R. W., 1966, Ann. Phys. (New York,), 37, 487
Martínez J., Pavón D., 1994, MNRAS, 268, 654
Mihalas D., Mihalas B., 1984, Foundations of Radiation Hydrodynamics. Oxford Univ. Press, Oxford
Nobili L., Turolla R., Zampieri L., 1993, ApJ, 404, 686
Ruderman M., 1972, ARA&A, 10, 427
Santos N. O., 1984, Phys. Lett. A, 106, 296
Santos N. O., 1985, MNRAS, 216, 403
Sawyer R. F., Scalapino D. J., 1973, Phys. Rev. D, 7, 953
Shapiro S. L., Teukolsky S. A., 1983, Black Holes, White Dwarfs and Neutron Stars. John Wiley & Sons, New York
Weinberg S., 1971, ApJ, 168, 175